Identification of mouse *trp* homologs and lipid rafts from spermatogenic cells and sperm

Claudia L. Treviño[a], Carmen J. Serrano[a,b], Carmen Beltrán[a], Ricardo Felix[b], Alberto Darszon[a,*]

[a] *Department of Genetics and Molecular Physiology, Institute of Biotechnology, UNAM, Avenida Universidad 2001, Col. Chamilpa, CP 62100, Cuernavaca, Mor., Mexico*
[b] *Department of Physiology, Biophysics and Neuroscience, Cinvestav-IPN, Mexico City, Mexico*

Received 17 October 2001; accepted 31 October 2001

First published online 15 November 2001

Edited by Maurice Montal

Abstract Intracellular Ca^{2+} has an important regulatory role in the control of sperm motility, capacitation, and the acrosome reaction (AR). However, little is known about the molecular identity of the membrane systems that regulate Ca^{2+} in sperm. In this report, we provide evidence for the expression of seven *Drosophila* transient receptor potential homolog genes (*trp*1–7) and three of their protein products (*Trp*1, *Trp*3 and *Trp*6) in mouse sperm. Allegedly some *trp*s encode capacitative Ca^{2+} channels. Immunoconfocal images showed that while *Trp*6 was present in the postacrosomal region and could be involved in sperm AR, expression of *Trp*1 and *Trp*3 was confined to the flagellum, suggesting that they may serve sperm to regulate important Ca^{2+}-dependent events in addition to the AR. Likewise, one of these proteins (*Trp*1) co-immunolocalized with caveolin-1, a major component of caveolae, a subset of lipid rafts potentially important for signaling events and Ca^{2+} flux. Furthermore, by using fluorescein-coupled cholera toxin B subunit, which specifically binds to the raft component ganglioside GM1, we identified caveolin- and *Trp*-independent lipid rafts residing in the plasma membrane of mature sperm. Notably, the distribution of GM1 changes drastically upon completion of the AR. © 2001 Published by Elsevier Science B.V. on behalf of the Federation of European Biochemical Societies.

Key words: Ca^{2+} channel; *trp*; Caveolin; Lipid raft; Sperm; Spermatogenic cell

1. Introduction

Diverse studies in mammalian sperm indicate that an increase in the concentration of intracellular Ca^{2+} ($[Ca^{2+}]_i$) is critical for several physiological processes during fertilization, such as sperm motility, capacitation and acrosome reaction (AR) [1]. Flagellar movement is activated when sperm are released from the caudal epididymis and cells become hyperactivated after insemination to confer sperm the capacity to detach from the oviductal mucosa and penetrate the egg's zona pellucida (ZP) [2–5]. During hyperactivation $[Ca^{2+}]_i$ undergoes fluctuations mainly in the midpiece of sperm flagellum, which are associated to oscillations in the frequency of the flagellar beat cycle [3]. In addition, $[Ca^{2+}]_i$ increases during capacitation, a crucial event that renders sperm the ability to fertilize an egg. Extracellular Ca^{2+} is one of the necessary constituents for the completion of capacitation of sperm in vitro [6]. Lastly, recent investigations show that the influx of Ca^{2+} in mammalian sperm during the ZP-induced AR occurs in two temporally distinct phases [7]: a fast transitory response followed by a much slower elevation in $[Ca^{2+}]_i$ which remains high while the agonist of the AR is present. Capacitation must precede AR, however hyperactivation and AR can occur independently, therefore either the two events are driven by different Ca^{2+} regulatory pathways and/or they are separated by subcellular compartmentalization. The latter hypothesis is possible in sperm because AR occurs in the rostrum of the head and hyperactivation in the flagellum.

In many cells the emptying of Ca^{2+} stores generates a gating signal that couples intracellular Ca^{2+} release to the opening of store-operated channels (SOCs) in the plasma membrane. Mammalian sperm possess SOCs, which have been proposed to be responsible for the sustained $[Ca^{2+}]_i$ elevation necessary for the AR ([7,8] reviewed in [1]). It has been proposed that the *Drosophila* transient receptor potential (*trp*) gene might code SOCs [9]. A total of seven mammalian *trp* homologs have been identified [10–12], five of them (mouse *trp*1, 3, 4, 5 and 6) have been detected in the testis [12–14]. Recently, Jungnickel and coworkers showed that *trp*2 localizes to the sperm head and is important for the sustained Ca^{2+} influx that drives the AR [15].

The plasma membrane contains microdomains called lipid rafts [16]. Raft microdomains can gather into clusters and have been shown to play important roles in the activation of signaling cascades in distinct cell types. It has been shown that endogenous *Trp*1 in human submandibular gland (HSG) cells is assembled in a multimeric complex of Ca^{2+} signaling proteins that includes the inositol 1,4,5-trisphosphate receptor type 3 (IP3R3), caveolin-1 (cav1) and the protein Gq/11 [17]. These findings indicate that SOC regulation may be a complex process, involving *Trp* interactions with other scaffolding or regulatory proteins.

Although hyperactivation, capacitation and the AR require extracellular Ca^{2+}, not much is known about the molecular identity and regulation of the Ca^{2+} transporters responsible for these fundamental processes. We therefore thought it pertinent to investigate the expression, distribution and possible molecular interactions of mammalian *Trp* homologs in mouse sperm as an initial step to assess the structural elements of Ca^{2+} entry channels in these cells.

*Corresponding author. Fax: (52)-73-17 23 88.
E-mail address: darszon@ibt.unam.mx (A. Darszon).

0014-5793/01/$20.00 © 2001 Published by Elsevier Science B.V. on behalf of the Federation of European Biochemical Societies.
PII: S0014-5793(01)03134-9

Table 1
Sets of primers designed to amplify mammalian *trp* homologs from mouse spermatogenic cells and the predicted sizes and melting temperatures of the PCR products

Gene	Forward primer 5′–3′	Reverse primer 5′–3′	T_m °C/size bp
*trp*1	CGGAATTCTGGATTATTGGGATGATTTGG	CGGGATCCYCKHGCAAYTTCCAYTC	52/705
*trp*2	CTGCGGAATGTGGAAGAGTCTG	AGGGCAATGTACTGAGGCTTAAACT	52/590
*trp*3	GGAATGATGTGGTCTGAATGTAAA	TAGCCCCAAGGTAGTAAGAATAAAGTA	52/478
*trp*4	TACAATACAGTCAGCCAACG	TCCTCCAAGGGTCACAAT	54/812
*trp*5	AAGCACTCTTCGCAATA	CTCGCAAACTTCCACTC	52/493
*trp*6	AGTTCCTCGTGGTCCTT	CTTTACATTCAGCCCATA	52/318
*trp*7	TGCTGCTCAAGGGTGC	CTGCTGACAGTTAGGGT	52/443

2. Materials and methods

2.1. Cell preparation

Spermatogenic cells were obtained as described elsewhere [18]. Briefly, testes of adult CD1 mice were decapsulated and subjected to enzymatic digestion (collagenase/trypsin) in EKRB solution, containing in mM: 120 NaCl, 25.2 $NaHCO_3$, 4.8 KCl, 1.2 KH_2PO_4, 1.2 $MgSO_4$, 1.3 $CaCl_2$, and 11 glucose. Cells were collected and resuspended in 0.5% bovine serum albumin (BSA)/EKRB, and filtered through a 80 μm nylon mesh. Aliquots of this cell suspension were taken for immunocytochemistry experiments (see below). For PCR experiments, the cell suspension was sedimented at unit gravity using a 2–4% BSA/EKRB linear gradient. After sedimentation, 10 ml fractions were collected and cell identity was determined by bright field microscopy. In addition, mouse sperm were collected from caput epididymis excised from adult CD1 mice. Cells were transferred to a 35 mm culture dish and allowed to exude in Medium 199 (Sigma Chemical Co., St. Louis, MO, USA) supplemented with 0.2% BSA, 0.22% $NaHCO_3$ and sodium pyruvate (30 mg/ml), fixed with 4% formaldehyde and dispensed onto slides as detailed below.

2.2. RNA isolation and RT-PCR experiments

RNA from isolated spermatogenic cells was extracted using RNAzol (Life Technologies Inc., Frederick, MD, USA) according to the manufacturer's instructions. The superscript system (Life Technologies) was used for reverse transcription polymerase chain reaction (RT-PCR). Total RNA was digested with RNAse-free DNase and 5 μg was reverse transcribed using random primers (Table 1). The resulting cDNA was used for amplification of the seven genes for the *trp* mammalian homologs. The 50 μl PCR reaction mixture contained: 0.25 mM each dNTP, 20 mM Tris buffer, 50 mM KCl, 1.5 mM $MgCl_2$, 0.1 μM each primer, 2.5 U *Taq* DNA polymerase, and 1 μl of reverse transcription reaction. Following an initial treatment for 5 min at 94°C, the following cycle was repeated 40 times: 30 s at 94°C, 1 min at 52/54°C (depending on the set of primers employed), and 30 s at 72°C. Final extension was 5 min at 72°C. cDNA fragments amplified by PCR were analyzed in a 1% agarose gel, cloned into pBluescript SK+/pPCR-ScriptAmpSK+ (Stratagene, La Jolla, CA, USA) and subsequently sequenced by the dideoxy chain termination method.

2.3. Immunolocalization

Aliquots (100 μl) of washed, diluted (1×10^6 cells/ml) mouse spermatogenic cell suspension were dispensed onto glass slides coated with a bioadhesive (Electron Microscopy Sciences, Ft. Washington, PA, USA) and allowed to settle for 30–60 min. Settled cells were immediately fixed with formaldehyde (4% final concentration) for 10 min, rinsed in PBS (3×5 min), and blocked with 2% BSA (in PBS) for 1–2 h. Samples were then incubated overnight at room temperature with primary antibodies (Table 2). After rinsing with PBS (3×5 min), samples were incubated for 1 h at room temperature with Alexa-conjugated secondary antibodies (Table 2), and subsequently rinsed again with PBS (3×5 min). Mouse mature sperm were processed in the same manner except for permeabilization with 0.1% Triton X-100 in PBS for 10 min after fixation. In addition, control experiments were processed likewise except by replacing the primary antibody with a peptide-blocked antibody prepared by incubation with its corresponding peptide. Fluorescence images were acquired with a confocal microscope using Comos 7.0 software (Bio-Rad Microscience, Hercules, CA, USA). Images were analyzed using Confocal Assistant software (Bio-Rad). To enable comparison, all images were recorded using the same parameters of laser power and photomultiplier sensitivity. Images shown are representative of at least three separate experiments in each condition and were processed by using identical values for contrast and brightness.

2.4. Cholera toxin B subunit-FITC labeling

Sperm were obtained as described above and three different samples were prepared as follows: (a) non-capacitated, handling cells in a non-capacitating medium (i.e. without BSA, $NaHCO_3$ and Ca^{2+}); (b) capacitated, by 30 min incubation at 37°C in capacitating medium; and (c) acrosome reacted cells, after capacitation cells were incubated for 30 min in the presence of 15 μM A23187 (Sigma). An aliquot of each sample was incubated for 30 min with 10 μg/ml cholera toxin B subunit conjugated to FITC (Sigma) in PBS with 0.1% BSA at 16°C. After treatment, cells were washed with PBS (3×5 min). For fixation cells were then treated with 4% paraformaldehyde in PBS for 10 min at room temperature and washed with PBS (3×5 min). At this point cells were analyzed using a confocal microscope or used for antibody staining as described earlier.

2.5. Western immunoblotting

Sperm were collected as described above using free Ca^{2+} Green medium (in mM: 4 KCl, 140 NaCl, 10 glucose, 25 HEPES, 4 EGTA, 2 $MgCl_2$ pH 7.5) and centrifuged in a 90% Percoll cushion for 10 min at $4000\times g$. The cells were recovered from the interface, washed with Green medium and centrifuged for 10 min at $1000\times g$. The pellet was resuspended in lysis buffer (100 mM Tris–HCl pH 8.0, 1 mM $MgCl_2$, 0.1 M PMSF, 1 μg/μl aprotinin) and frozen at −80°C for at least 1 h. Cell lysates were thawed, homogenized in a Dounce homogenizer and diluted into sucrose buffer (in mM: 250 sucrose, 10 Tris–HCl, 20 HEPES, 1 DTT and 1 μg/μl aprotinin, pH 7.5). The homogenate was centrifuged at $3000\times g$ for 15 min at 4°C and the supernatant was then spun down at $70\,000\times g$ for 15 min at 4°C. The pellet containing the membranes was resuspended in loading buffer and subjected to sodium dodecyl sulfate–polyacrylamide gel electrophoresis (SDS–PAGE) and Western blotting. Anti-caveolin antibody (Santa Cruz Biotechnology, Inc., Santa Cruz, CA, USA) was diluted

Table 2
Specific antibodies

Antibody	Source	Supplier	Dilution
*Trp*1	rabbit	Alomone Labs (Jerusalem, Israel)	1/80
*Trp*3	rabbit	Alomone Labs (Jerusalem, Israel)	1/100
*Trp*6	rabbit	Alomone Labs (Jerusalem, Israel)	1/100
Caveolin-1	rabbit	Santa Cruz Biotechnology (La Jolla, CA, USA)	1/200
Alexa 488	rabbit	Molecular Probes Inc. (Eugene, OR, USA)	1/100
Alexa 592	rabbit	Molecular Probes Inc. (Eugene, OR, USA)	1/100

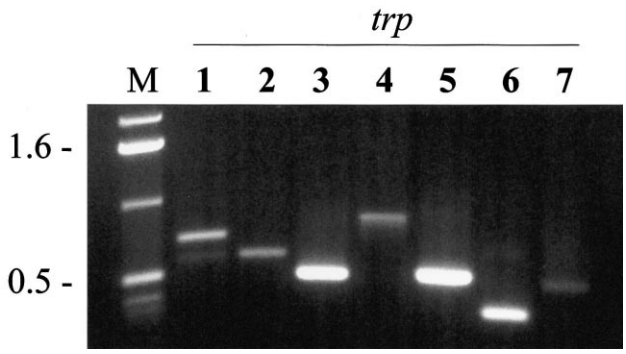

Fig. 1. Expression of mouse *trp* homologs from spermatogenic cells. Identification of seven different *trp*-related amplifications (lanes 1–7) of RT-PCR from mouse spermatogenic cells. Products were sequenced to verify specific amplification and corresponded to mouse *trp* homologs, *mtrp*1–7. *M* denotes molecular weights of the standards on the left.

1:500 and the control reaction was performed by incubation of the primary antibody with a four-fold excess of the antigenic peptide. Signals were obtained with ECL reagents and exposed to Hyperfilm-βmax (Amersham Pharmacia Biotech., Piscataway, NJ, USA).

3. Results

3.1. Trp channels in spermatogenic cells and sperm

In order to identify messenger RNAs encoding for the mammalian *trp* homologs, RT-PCR was performed on total RNA isolated from mouse spermatogenic cells using a selective and specific set of primers (see Table 1 for details) designed against the different *trp*s identified in other tissues and mammalian species. We tested seven pairs of primers and all of them amplified products corresponding to the predicted sizes for *trp* homologs (*trp*1–7; Fig. 1). The identity of these products was further confirmed by subsequent sequencing.

Having shown molecular evidence for the presence of the seven genes encoding mammalian *trp* homologs in spermatogenic cells, we investigated the expression of distinct *Trp* at

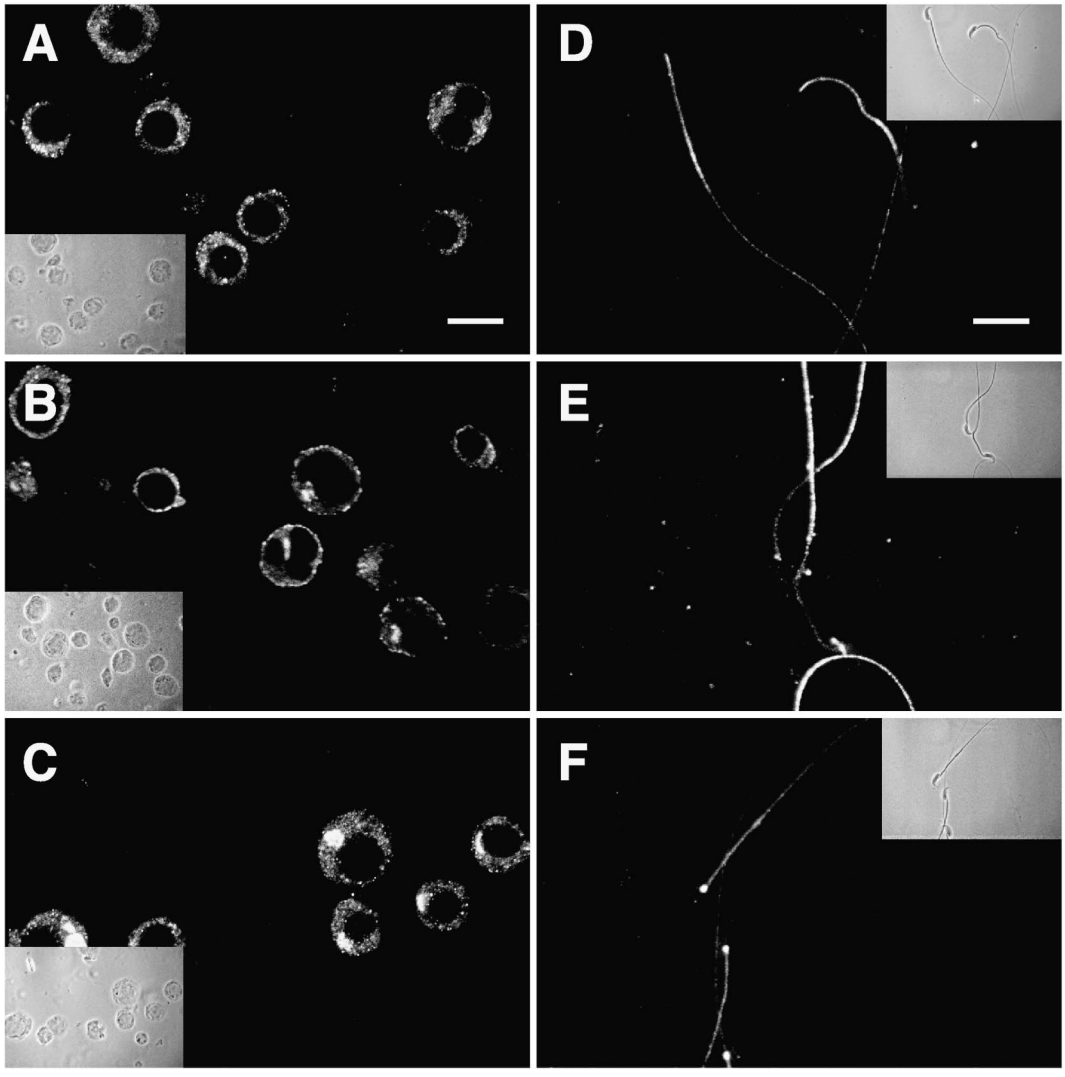

Fig. 2. Identification and immunolocalization of *Trp* proteins from mouse spermatogenic cells and sperm. A–C: Confocal fluorescence images of spermatogenic cells labeled with specific anti-*Trp*1, 3 and 6 antibodies, respectively, illustrating the pattern of staining (scale bar = 9 μm). The corresponding phase contrast images are shown in the inset to figures. D–E: Representative optical sections of mature sperm stained with the same anti-*Trp* antibodies indicating the presence of these proteins mainly in the cell surface of the flagellum (scale bar = 14 μm). Insets show the corresponding phase contrast photomicrographs.

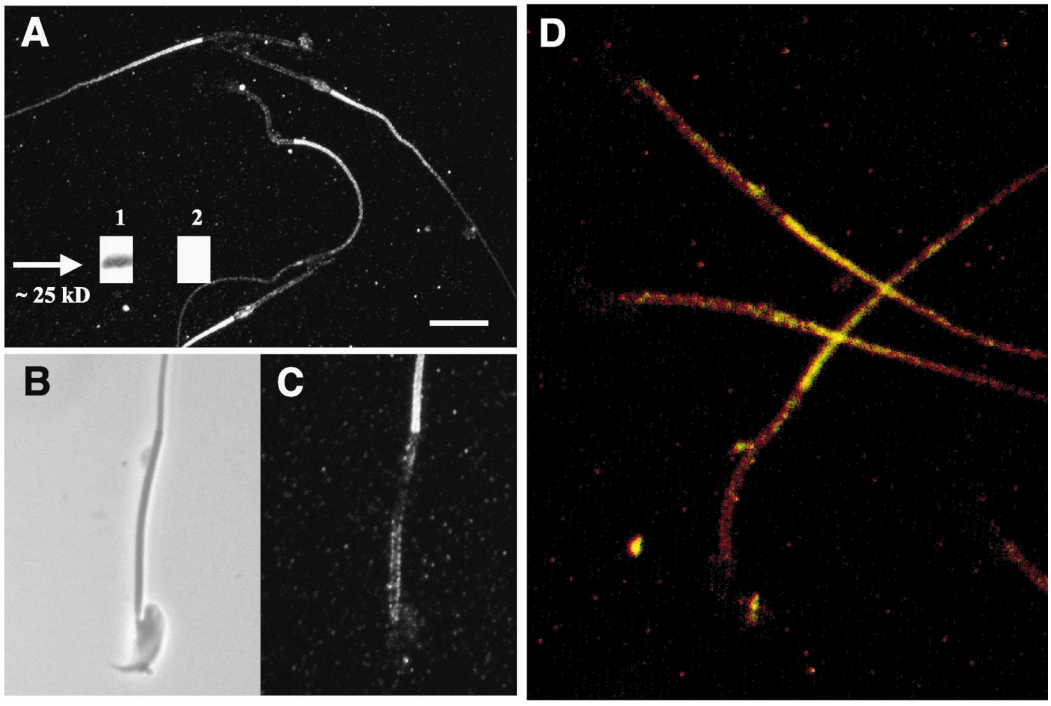

Fig. 3. Cav1 immunolocalization in mouse sperm. A: Confocal immunofluorescence image obtained from mature sperm treated with a specific anti-cav1 antibody (Table 2). Punctate immunostaining is predominant in the principal piece of the flagellum, although the midpiece is also labeled (scale bar = 16 μm). Inset: Membranes isolated from mature sperm were separated on SDS–PAGE, and analyzed by Western blotting with a polyclonal antibody against cav1 (lane 1). Control experiments using antibodies blocked by previous exposure to the peptide antigen exhibited no signal (lane 2). C: Representative image at higher magnification of mouse mature sperm treated with the same anti-cav1 antibody. B is the phase contrast image of C. D: Co-localization of *Trp*1 (shown as green), and cav1 (shown as red) in mouse sperm. An enlarged overlay of images is presented.

the protein level in mouse spermatogenic cells as well as in mature sperm. We used antibodies raised against *Trp*1, 3 and 6 (see Table 2 for details), whose specificity has been tested previously [19–21]. Unfortunately, this analysis did not include *Trp*2, 4, 5 and 7 because specific antibodies directed to these proteins are not available. Fig. 2A shows a confocal immunofluorescence image of spermatogenic cells treated with antibodies against *Trp*1. As can be seen, immunostaining is diffusely distributed throughout the cytoplasm. These data give a true picture of the *Trp*1 localization in spermatogenic cells, since using the specific primary antibody blocked with the peptide antigen showed negligible fluorescence staining (not shown). Specific immunoreactivity was punctuate presumably corresponding to clusters of *Trp*1, and the nuclei excluded staining. Similar results were obtained when the *Trp*3 antibody was used (Fig. 2B). In this case the immunoreactivity was also diffuse and evenly distributed throughout the cytoplasm. However, a more peripheral pattern of *Trp*3 distribution clearly indicates that a fraction of this protein is localized at the plasma membrane. Fig. 2C illustrates a representative immunoimage obtained at a focal plane that offers a useful representation of the overall distribution of *Trp*6 in spermatogenic cells. Here, the relatively low-magnification image reveals again that immunoreactivity was diffusely distributed in the cytoplasm. However, in most of the cells *Trp*6 seemed to be localized in a confined region, suggesting that the label might be specifically associated with a particular membrane system or cytoplasmic structure such as the Golgi network. Further studies will be needed to determine the precise localization of these *Trp*6 clusters in which the use of Golgi markers may be useful. As in the case of *Trp*1 and 3, control experiments using *Trp*6 antibodies blocked by previous exposure to the peptide antigen exhibited very low residual staining (not shown).

Fig. 2D–F show representative immunoimages of *Trp* staining in mature sperm. *Trp*1 and 3 were detected mainly at the flagellum with a punctuate pattern. *Trp*1 puncta were distributed mostly to the midpiece (Fig. 2D) while those of *Trp*3 were more intense in the distal segment of the flagellum (Fig. 2E). The control experiments using antibodies blocked by previous exposure to the peptide antigen showed only very low fluorescence, indicating a high level of specificity in the detected signal. Fig. 2F allows examination of the head and flagellum. As can be seen, *Trp*6 staining showed a peculiar expression pattern. A dense spot localized in the neck of sperm was consistently observed in most of the cells examined. This pattern agrees with the regional localization of *Trp*6 observed in spermatogenic cells. In addition, although a signal is also present in the flagellum, *Trp*6 seemed to be expressed at a very low density in this region, or not at all, since immunostaining was only partially blocked by the corresponding antigen fusion protein (not shown).

3.2. Lipid rafts and transduction complexes

As mentioned earlier, some *Trp*s are strong candidates to form SOCs in different mammalian species, though the detailed protein composition and regulation of SOCs is still ill defined [22–24]. *Trp*s have been detected in specialized lipid domains (lipid rafts) [24]. To begin to elucidate the determinants of the localization and regulation of sperm *Trp*s, we

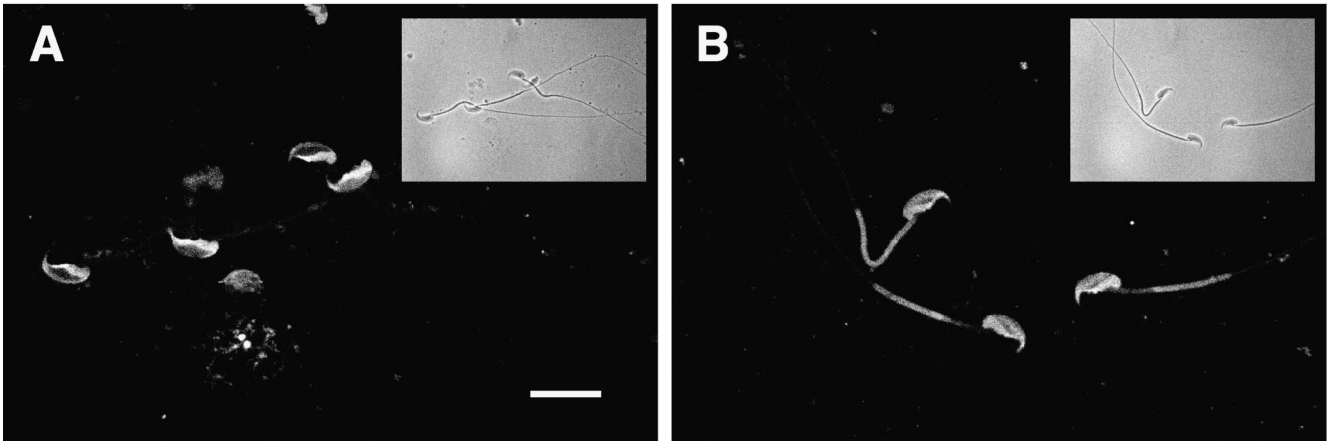

Fig. 4. Redistribution of lipid rafts after sperm acrosome reaction. A: Representative confocal immunofluorescence image of FITC-CTX distribution in capacitated sperm, showing the fluorescence signal confined to the cell surface of sperm's head. B: Redistribution of FITC-CTX to the sperm flagellum after the induction of the acrosome reaction with the Ca^{2+} ionophore A23187 (scale bar = 11 μm). Insets represent the corresponding phase contrast images.

investigated the possible molecular interactions between them and caveolin-1 (cav1), a specific marker of lipid rafts. Fig. 3A shows representative confocal immunofluorescence cav1 images in mouse mature sperm indicating that the fluorescence staining is localized to discrete regions of the sperm flagellum. In this case, staining is both smooth and punctuate in appearance and more intense in the surface of the principal piece. In addition to this region the cav1 antibody stained also the midpiece of the flagellum with a punctuate pattern (Fig. 3C) but with much less intensity. In some cases cav1 also stained the sperm's head, but this signal could not be reproduced consistently. Control experiments (not shown) revealed very low fluorescence, indicating that the detected signal is highly specific. This is confirmed by the detection of endogenous cav1 by Western immunoblotting of sperm membranes, as shown in the inset to Fig. 3A. Therefore, this study provides what is to our knowledge the first evidence for the presence of cav1 in mouse mature sperm.

Having established the presence of cav1 in mouse sperm, we next compared its localization with that of the *Trp* proteins by

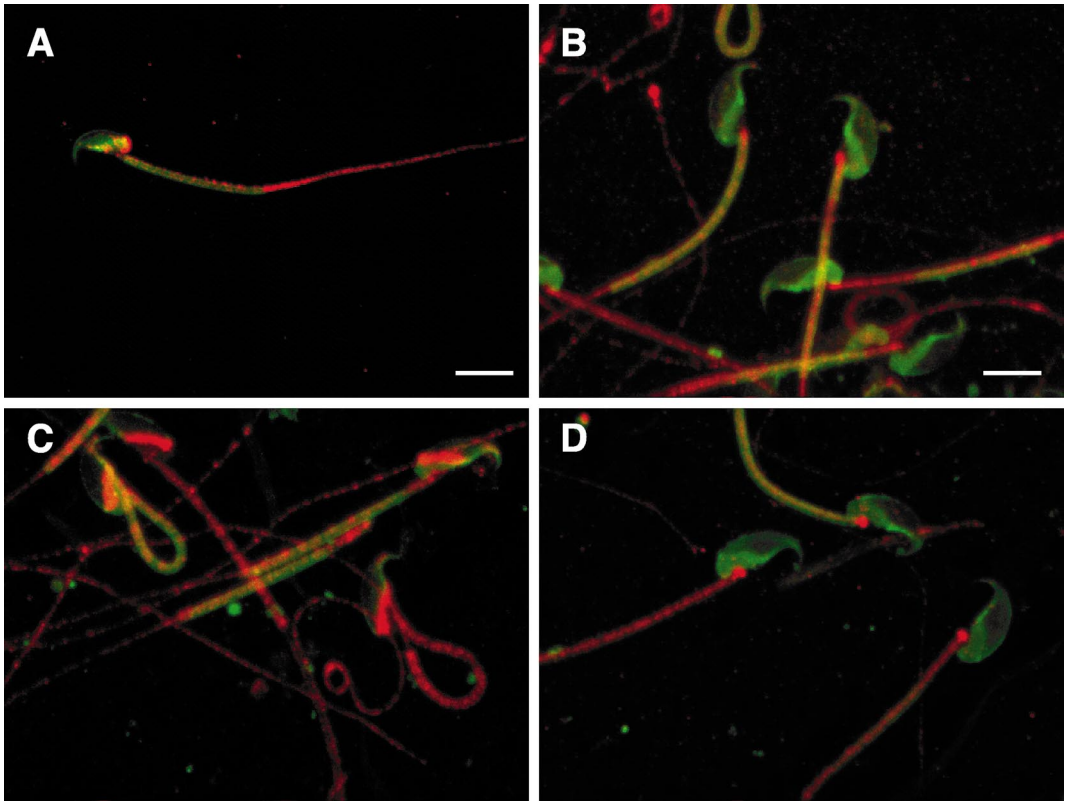

Fig. 5. Localization by double immunofluorescence of FITC-CTX, cav1 and *Trp*s. A: Mouse mature sperm stained using FITC-CTX and a polyclonal antibody against cav1 (shown as red). The difference in the distribution of both markers is illustrated by the overlay of both images. B–D: Sperm immunostained using FITC-CTX corresponding to raft glycosphingolipid GM1 and polyclonal antibodies against *Trp*1, 3 and 6, respectively (shown as red). Scale bar in A: 8 μm, in B: 5.5 μm.

double staining using the antibodies listed in Table 2. Fig. 3D shows the combined image of the localization of cav1 and the *Trp*1. High expression levels of both proteins are found in the sperm flagellum. Interestingly, the expressions of cav1 and *Trp*1 closely overlap in the middle region of the flagellum but not in the distal flagellar segment. Although the localizations of cav1 and *Trp*3 are similar, there is no appreciable overlapping of the signals (not shown). In addition, immunofluorescences for cav1 and Trp6 do not appear to co-localize whatsoever (not shown). These results are consistent with the idea that *Trp*1 is assembled in a signaling complex associated with caveolin-scaffolding lipid raft domains [24]. Further co-immunoprecipitation experiments will be required to corroborate the possible molecular interaction between these two proteins in mature mouse sperm.

It is known that during the process of capacitation, cholesterol is removed from the plasma membrane causing redistribution and/or insertion of membrane components [6]. Also during the AR, fusion of the acrosomal membrane with the plasma membrane exposes a surface with a unique composition. We asked whether the distribution of *Trp*s and cav1 (probably in lipid rafts) changed during capacitation and the AR, contributing to the Ca^{2+} influx regulation during these events. We compared the distribution of *Trp*1, *Trp*3, *Trp*6 and cav1, in non-capacitated, capacitated and acrosome reacted sperm. Unexpectedly, we did not detect any pattern changes of *Trp*s and cav1 proteins during these events (not shown). Therefore, we decided to use another raft marker, the fluorescein-conjugated cholera toxin B subunit (FITC-CTX). This toxin binds specifically to the raft component ganglioside GM1 [25], previously proven to be a component of mammalian sperm plasma membrane [26]. Interestingly, non-capacitated and capacitated sperm displayed the same dispersed pattern of FITC-CTX expression in the head (Fig. 4A), and no signal was detected in the flagellum. These results indicate that most of the GM1 is restricted to the sperm head and does not change during capacitation. Remarkably, during the sperm AR FITC-CTX labeling becomes apparent also in the midpiece of sperm flagellum (Fig. 4B). These changes in sperm plasma membrane composition might be involved in the acquisition of the capability to bind to the extracellular matrix of the egg and develop the AR.

We then sought to determine whether the cholera toxin B subunit co-localized with *Trp*s or cav1 by double staining sperm with FITC-CTX and the corresponding polyclonal antibodies. For these co-localization experiments acrosome reacted sperm were chosen, because only in this condition FITC-CTX binds to the flagella. Cav1 staining was found more abundantly over the distal region of the flagellum and did not co-localize with FITC-CTX (Fig. 5A). In addition, to assess the differential distribution of FITC-CTX and the *Trp* proteins over the cell surface, confocal midsection images of mature sperm were analyzed. *Trp*1, 3 and 6 immunostaining distribution was identical to that we had previously observed (Fig. 2D–F). However, as shown in Fig. 5B, C and D, we did not detect co-localization between *Trp*1, 3 and 6 with FITC-CTX. Although *Trp*1 and *Trp*3 are also found in flagellum, staining was sharply separated at the cell surface in the sperm's tail. Therefore, segregation of the *Trp*s and ganglioside GM1 was independent from the antibody combination used. Taken as a whole these experiments suggest that different lipid raft components in the plasma membrane on mouse mature sperm exhibit different patterns of distribution with *Trp* proteins ranging from a high degree of co-localization of *Trp*1 and cav1 to a complete segregation in the case of ganglioside GM1.

4. Discussion

This report reveals that all *trp* known genes are expressed in spermatogenic cells. The presence of multiple types of *trp* mammalian homologs in mouse spermatogenic cells and sperm extends the diversity of Ca^{2+} channel subtypes present in these cells and provides the basis for their functional versatility. Notably, we found that only one of their protein products (*Trp*6) is localized in the vicinity of the sperm head, while *Trp*1 and *Trp*3 are present mainly in the flagellum suggesting unexpected physiological roles for *Trp*s in sperm.

The function of the different sperm *Trp*s is unknown; those found in the flagellum could participate in important events such as the initiation of motility (activation) and hyperactivation, which are important for fertilization [3]. Though little is known about the pathways that regulate these processes, Ca^{2+} influx has been implicated as a prerequisite to initiate sperm activation and hyperactivation [2–4]. Activation is the flagellar movement initiated when mature sperm are released from the caudal epididymis. Hyperactivation is characterized by an increase in the amplitude of flagellar beating and it is a reversible event, as opposed to the irreversibility of the AR. The molecular entities that regulate these two processes are probably distinct. $[Ca^{2+}]_i$ increases in hyperactivated sperm in the acrosomal region, postacrosomal region and to a greater extent in the flagellar midpiece. Perhaps this is because the main region of Ca^{2+} influx during hyperactivation is the flagellum [2,3]. The switch that turns on hyperactivation is unknown, but presumably it involves a signaling pathway that elevates $[Ca^{2+}]_i$. Though different types of voltage-gated Ca^{2+} channels are present in sperm flagella and are likely to contribute to the rise in $[Ca^{2+}]_i$ (reviewed in [27]), *Trp* proteins could also participate in this event. Interestingly, the redundant nuclear envelope (RNE), a poorly characterized sperm structure, that localizes caudal to the posterior ring at the region of the sperm head, has been recently proposed to associate with the annulate lamellae and probably functions as a specialized endoplasmic reticulum [28]. Possibly local Ca^{2+} release from the RNE could activate flagellar *Trp*s. Alternatively, other *Trp* regulators present in sperm such as diacylglycerol, polyunsaturated fatty acids, calmodulin (CaM), calpactin, calsequestrin and calreticulin, could modulate these channels and influence motility [29–32]. Interestingly, it has been shown recently that mammalian *Trp*4 binds CaM in a Ca^{2+}-dependent way [33].

The ZP-induced AR involves at least two different Ca^{2+} channels: (1) a voltage-gated Ca^{2+} channel whose opening produces a fast transient Ca^{2+} influx, and (2) a SOC that is activated as a result of IP3 production and stimulation of the IP3 receptor. *Trp*2 has been identified as a component of the ZP-regulated SOC activated during the AR [15]. However, the functional channel may be composed of different *Trp* proteins [13]. In this regard *Trp*6 could participate in processes requiring Ca^{2+} uptake during the AR.

Given the various potential roles *Trp*s may play in sperm physiology, a detailed understanding of their regulation and location in specialized lipid domains, and the interactions between themselves and other Ca^{2+} signaling proteins, is re-

quired. Lipid microdomains represent potential specialized sperm–egg interaction sites as well as platforms for different signal transduction components such as Ca^{2+} signaling proteins. We showed the presence of independent cav1 and GM1 lipid rafts in the sperm membrane. Cav1 domains co-localize with *trp*1 and GM1 changes its distribution upon completion of the AR. These findings suggest that these lipid microdomains may participate during important events in sperm physiology. A complete characterization of lipid rafts in the sperm membrane is an important goal in future studies.

Acknowledgements: This work was supported by grants from DGAPA IN201599 (UNAM) to A.D. and C.L.T. and from CONACyT 27707-N to A.D., 32052-N to C.B. and 31735-N to R.F. C.J.S. is a recipient of a CONACyT postdoctoral fellowship. We thank X. Alvarado, E. Bustos, S. González, R. Hernández, E. Mata, M. Olvera and A. Vega-Hernández for expert technical assistance.

References

[1] Darszon, A., Labarca, P., Nishigaki, T. and Espinosa, F. (1999) Physiol. Rev. 79, 481–510.
[2] Suarez, S.S., Varosi, S.M. and Dai, X. (1993) Proc. Natl. Acad. Sci. USA 90, 4660–4664.
[3] Suarez, S.S. and Dai, X. (1995) Mol. Reprod. Dev. 42, 325–333.
[4] Suarez, S.S. (1996) J. Androl. 17, 331–335.
[5] Stauss, C.R., Votta, T.J. and Suarez, S.S. (1995) Biol. Reprod. 53, 1280–1285.
[6] Baldi, E., Luconi, M., Bonaccorsi, L., Muratori, M. and Forti, G. (2000) Front. Biosci. 5, E110–E123.
[7] O'Toole, C.M., Arnoult, C., Darszon, A., Steinhardt, R.A. and Florman, H.M. (2000) Mol. Biol. Cell 11, 1571–1584.
[8] Santi, C.M., Santos, T., Hernandez-Cruz, A. and Darszon, A. (1998) J. Gen. Physiol. 112, 33–53.
[9] Montell, C. (1997) Mol. Pharmacol. 52, 755–763.
[10] Putney Jr., J.W. and McKay, R.R. (1999) Bioessays 21, 38–46.
[11] Boulay, G., Brown, D.M., Qin, N., Jiang, M., Dietrich, A., Zhu, M.X., Chen, Z., Birnbaumer, M., Mikoshiba, K. and Birnbaumer, L. (1999) Proc. Natl. Acad. Sci. USA 96, 14955–14960.
[12] Vannier, B., Peyton, M., Boulay, G., Brown, D., Qin, N., Jiang, M., Zhu, X. and Birnbaumer, L. (1999) Proc. Natl. Acad. Sci. USA 96, 2060–2064.
[13] Okada, T., Inoue, R., Yamazaki, K., Maeda, A., Kurosaki, T., Yamakuni, T., Tanaka, I., Shimizu, S., Ikenaka, K., Imoto, K. and Mori, Y. (1999) J. Biol. Chem. 274, 27359–27370.
[14] García, R. and Schilling, W. (1997) Biochem. Biophys. Res. Commun. 239, 279–283.
[15] Jungnickel, M.K., Marrero, H., Birnbaumer, L., Lemos, J.R. and Florman, H.M. (2001) Nat. Cell Biol. 3, 499–502.
[16] Simons, K. and Toomre, D. (2000) Nat. Rev. 1, 31–39.
[17] Lockwich, T.P., Liu, X., Singh, B.B., Jadlowiec, J., Weiland, S. and Ambudkar, I.S. (2000) J. Biol. Chem. 275, 11934–11942.
[18] Serrano, C.J., Treviño, C.L., Felix, R. and Darszon, A. (1999) FEBS Lett. 462, 171–176.
[19] Zhu, X., Jiang, M., Peyton, M., Boulay, G., Hurst, R., Stefani, E. and Birnbaumer, L. (1996) Cell 85, 661–671.
[20] Mori, Y., Takada, N., Okada, T., Wakamori, M., Imoto, K., Wanifuchi, H., Oka, H., Oba, A., Ikenaka, K. and Kurosaki, T. (1998) Neuroreport 9, 507–515.
[21] Zhu, X., Chu, P.B., Peyton, M. and Birnbaumer, L. (1995) FEBS Lett. 373, 193–198.
[22] Braun, F.J., Broad, L.M., Armstrong, D.L. and Putney Jr., J.W. (2001) J. Biol. Chem. 276, 1063–1070.
[23] Liu, X., Wang, W., Singh, B.B., Lockwich, T.P., Jadlowiec, J., O'Connell, B.C., Wellner, R.B., Zhu, M.X. and Ambudkar, I.S. (2000) J. Biol. Chem. 275, 3403–3411.
[24] Kiselyov, K., Xu, X., Mozhayeva, G., Kuo, T., Pessah, I., Mignery, G., Zhu, X., Birnbaumer, L. and Muallem, S. (1998) Nature 396, 478–482.
[25] Harder, T., Scheiffele, P., Verkade, P. and Simons, K. (1998) J. Cell Biol. 141, 929–942.
[26] Gore, P.J., Singh, S.P. and Brooks, D.E. (1986) Biochim. Biophys. Acta 876, 36–47.
[27] Darszon, A., Beltrán, C., Félix, R., Nishigaki, T. and Treviño, C.L. (2001) Dev. Biol., in press.
[28] Westbrook, V.A., Diekman, A.B., Naaby-Hansen, S., Coonrod, S.A., Klotz, K.L., Thomas, T.S., Norton, E.J., Flickinger, C.J. and Herr, J.C. (2001) Biol. Reprod. 64, 345–358.
[29] Si, Y. and Olds-Clarke, P. (2000) Biol. Reprod. 62, 1231–1239.
[30] Berruti, G. (1988) Exp. Cell. Res. 179, 374–384.
[31] Berruti, G. and Porzio, S. (1990) Eur. J. Cell Biol. 52, 117–122.
[32] Nakamura, M., Oshio, S., Tamura, A., Okinaga, S. and Arai, K. (1992) Biochem. Biophys. Res. Commun. 186, 984–990.
[33] Trost, C., Bergs, C., Himmerkus, N. and Flockerzi, V. (2001) Biochem. J. 355, 663–670.